

Accepted Manuscript

Synthesis, characterization and photophysical properties of new cyclometallated platinum(II) complexes with pyrazolonate ancillary ligand

Yulya E. Begantsova, Leonid N. Bochkarev, Sergei Yu. Ketkov, Evgenii V. Baranov, Mikhail N. Bochkarev, Dmitry G. Yakhvarov



PII: S0022-328X(13)00156-3

DOI: [10.1016/j.jorganchem.2013.02.027](https://doi.org/10.1016/j.jorganchem.2013.02.027)

Reference: JOM 17902

To appear in: *Journal of Organometallic Chemistry*

Received Date: 25 December 2012

Revised Date: 14 February 2013

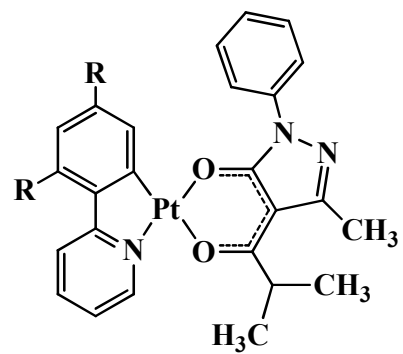
Accepted Date: 21 February 2013

Please cite this article as: Y.E. Begantsova, L.N. Bochkarev, S.Y. Ketkov, E.V. Baranov, M.N. Bochkarev, D.G. Yakhvarov, Synthesis, characterization and photophysical properties of new cyclometallated platinum(II) complexes with pyrazolonate ancillary ligand, *Journal of Organometallic Chemistry* (2013), doi: 10.1016/j.jorganchem.2013.02.027.

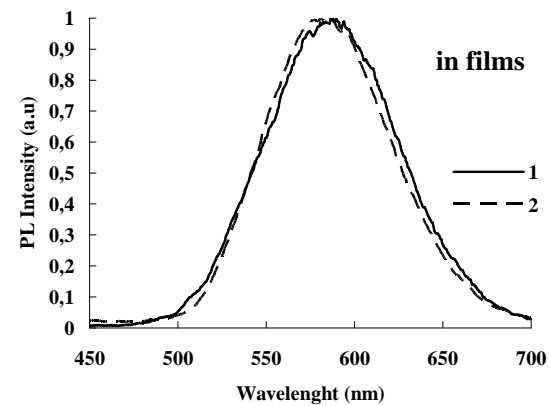
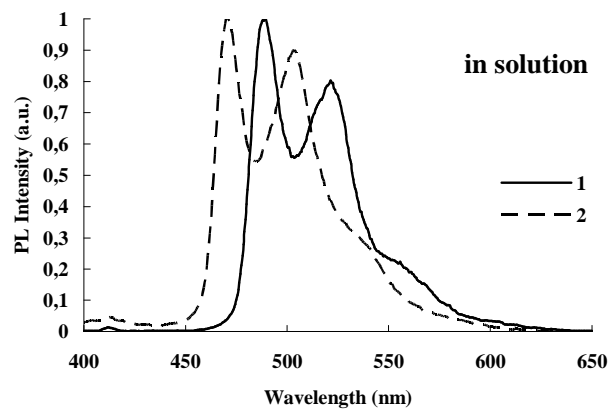
This is a PDF file of an unedited manuscript that has been accepted for publication. As a service to our customers we are providing this early version of the manuscript. The manuscript will undergo copyediting, typesetting, and review of the resulting proof before it is published in its final form. Please note that during the production process errors may be discovered which could affect the content, and all legal disclaimers that apply to the journal pertain.

Highlights

► New cyclometalated platinum(II) complexes with pyrazolonate ancillary ligand. ► The compounds are luminescent at room temperature both in solution and in solid state. ► X-ray analysis, electrochemical study and DFT calculations were performed. ► Computational study agree very well with the experimental data.



R = H (1); F (2)



Synthesis, characterization and photophysical properties of new cyclometallated platinum(II) complexes with pyrazolonate ancillary ligand

Yulya E. Begantsova^a, Leonid N. Bochkarev^{a*}, Sergei Yu. Ketkov^{ab}, Evgenii V. Baranov^a, Mikhail N. Bochkarev^a, Dmitry G. Yakhvarov^c

^aG.A. Razuvaev Institute of Organometallic Chemistry, Russian Academy of Sciences, Tropinin str.,49, Nizhny Novgorod, 603950, Russian Federation

^bDepartment of Chemistry, N.I. Lobachevsky Nizhny Novgorod State University, 23 Gagarin Avenue, Nizhny Novgorod, 603950, Russia Federation

^cA.M. Butlerov Institute of Chemistry, Kazan (Volga Region) Federal University, Kremlevskaya str., 18, Kazan, 420008, Russian Federation

Abstract

New cyclometalated platinum(II) complexes with pyrazolonate ancillary ligand (ppy)Pt(pmip) (**1**) and (dfppy)Pt(pmip) (**2**) (ppy = 2-phenylpyridine, dfppy = (4,6-difluorophenyl)pyridine, Hpmip = 1-phenyl-3-methyl-4-isobutyryl-5-pyrazolone) were synthesized and structurally characterized. Both compounds revealed square-planar geometry. The crystal cell of **1** was found to contain the monomer molecules of platinum compound whereas dimer molecules of **2** with short Pt...Pt contacts of 3.2217(3) Å were observed in the crystal cell of **2**. Photophysical properties of **1** and **2** were investigated in detail. The highly resolved photoluminescence spectra of the platinum complexes in solution contain emission bands in the region of 470-550 nm attributed to monomer compounds **1** and **2**. The triplet-state energies of **1** and **2** obtained from DFT calculations agree very well with the experimental data. In the crystalline state complex **2** revealed excimer emission as a structureless broad band at ca. 584 nm related to dimer molecules of platinum compound presented in the crystals.

Keywords: Cyclometalated platinum(II) complex, synthesis, structures, cyclic voltammetry, DFT calculation, photophysical properties

1. Introduction

* Corresponding author. Tel.: +7 (831) 4627010; fax: +7 (831) 4627497.
E-mail address: lnbo@iomc.ras.ru (L.N.Bochkarev).

Cyclometalated platinum(II) complexes are widely used as efficient emitters in OLEDs [1, 2]. The high efficiency of platinum based emitters is due to strong spin-orbit coupling of the heavy metal atom which allows for the facile intersystem crossing from the singlet to the triplet excited state. Thus both singlet and triplet excitons can be utilized in the platinum complexes and as a result their internal quantum efficiency can theoretically approach 100%. Square-planar platinum(II) luminescent complexes have a tendency to form aggregates in the solid state or in concentrated solution and can produce both high energy monomer emission and red-shifted broad-band excimer emission [1, 3, 4]. The relative intensity of monomer and aggregate emissions can be regulated by either dopant concentration of platinum complex in host matrix or by variation of the ligand environment around the platinum center [3-5]. Using these strategies the efficient single dopant white OLEDs (WOLEDs) have been successfully developed [2, 6, 7].

One of the most exploring type of platinum emitters comprises the complexes with cyclometalating arylpyridine ligands and ancillary β -diketonate ligands [1, 2]. In a series of works a large number of platinum complexes with the same β -diketonate ligand (mostly acac ligand) and different substituted arylpyridine ligands were synthesized and the relations between their luminescent properties and the nature of arylpyridine ligands were explored [4, 8-11]. The other representative works were devoted to synthesis and luminescent properties of platinum complexes with phenylpyridine or (4,6-difluorophenyl)pyridine ligands and different β -diketonate ancillary ligands [3, 5, 12-15]. The luminescent efficiency and ability to form aggregates and produce excimer emission were shown to depend both on the nature of cyclometalating arylpyridine ligands and ancillary β -diketonate ligands.

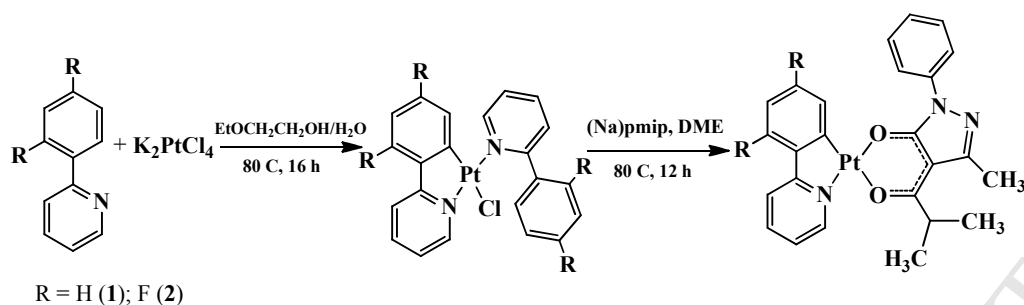
The preparation and efficient PL and EL properties of the platinum(II) complex with cyclometalating 1-phenylisoquinoline ligand and fluorine substituted pyrazolonate ancillary ligand have been recently described [16].

Herein we report the synthesis, characterization and photophysical properties of the new cyclometalated platinum(II) complexes **1** and **2** with arylpyridine and 1-phenyl-3-methyl-4-isobutyryl-5-pyrazolonate ligands.

2. Results and discussion

2.1. Synthesis

Platinum complexes **1** and **2** were synthesized by the reaction of cyclometalated Pt(II) chlorides with the sodium pyrazolonate reagent (Scheme 1).



Scheme 1. Synthetic route to the platinum complexes **1** and **2**.

The products **1** and **2** were isolated as air stable yellow and orange crystalline solids, respectively. They were characterized by IR and NMR spectroscopy, elemental analysis, and X-ray crystallography. NMR study revealed that both compounds exist as a mixture of two isomers (with the ratio of ~ 3:1) due to the different arrangement of the ligands around the Pt center. The complexes **1** and **2** exhibit high thermal stability. The onset decomposition temperature (T_d) for 5% weight loss is 308 °C for **1** and 242 °C for **2**.

2.2. Crystallography

X-ray crystal structure investigation of **1** revealed that Pt(1) atom had a square-planar coordination (Fig. 1, Tabl. 1). The sum of the angles at Pt(1) in the plane is 360°. Mean deviation of atoms O(1), O(2), N(3), C(25) and Pt(1) from the plane is 0.023 Å. The ppy ligand is disposed in one plane with the pmip ligand.

Fig. 1.

Table 1.

Crystal packing analysis established that in crystal of **1** the molecules of the Pt complex form a one-dimensional chain in a head-to-head manner (Fig. 2). The long intermolecular Pt...Pt distance (6.975 Å) indicates the absence of Pt...Pt interaction between molecules of **1** in crystal.

Fig. 2.

In contrast to **1**, complex **2** is a dimer and consists of two (dfppy)Pt(pmip) molecules linked to each other in a head-to-head fashion via the Pt(1) and Pt(2) atoms (Fig. 3).

Fig. 3.

The Pt(1)-Pt(2) distance (3.2217(3) Å) in **2** is larger than the sum of the covalent radii of Pt(II) (2.74 Å [17]), but significantly smaller than the sum of the Van der Waals radii of Pt (4.2 Å [17]) suggesting a Pt(1)...Pt(2) interaction in dimeric compound **2**. It should be noted that a

similar Pt...Pt interaction was found to exist in other dimeric monocyclometalated square-planar platinum(II) complexes with Pt-Pt distances lying in the range of 3.24-3.74 Å [9, 10].

Two (dfppy)Pt(pmip) molecules in dimer **2** are disposed in parallel orientation relatively to each other. The dihedral angle O(1)O(2)N(3)C(25)Pt(1) and O(3)O(4)N(6)C(50)Pt(2) is 2.7°. The Pt(1) and Pt(2) atoms have a square-planar geometry as in **1**. The sums of angles in the planes of Pt(1) and Pt(2) atoms are 359.9 and 360° respectively. Mean deviations of atoms O(1), O(2), N(3), C(25), Pt(1) and O(3), O(4), N(6), C(50), Pt(2) are 0.018 and 0.009 Å respectively.

Dimeric complex **2** has a skewed geometry. The torsion angles C(2)-Pt(1)-Pt(2)-C(27) and centroid(N(3),C(25))-Pt(1)-Pt(2)-centroid(N(6),C(50)) are 43.6° and 39.6°, respectively. The dfppy ligands of the two (dfppy)Pt(pmip) molecules in **2** are almost coplanar to each other, the angle between the dfppy planes is 3.5°. The short distance between two dfppy planes (3.390 Å) in **2** indicates a presence of the π - π interaction between the aromatic dfppy fragments [18].

Geometrical features of the pmip and ppy (dfppy) ligands in **1** and **2** are similar. The pmip ligands in **1** were found to differ from those in **2** by the orientations of the Ph-groups with respect to the pyrazolone fragments. The dihedral angle between the phenyl and pyrazolone rings is 31.4° in **1** and 9.8° (10.1°) in **2**.

The dimeric molecules in crystal of **2** are packed in the head-to-tail fashion (Fig. 4).

Fig. 4.

Intermolecular Pt...Pt distances between atoms Pt1A and Pt1B, Pt1C and Pt1D are equal to 5.331 Å, while the Pt2B...Pt2C distance is 5.018 Å. The observed distances are substantially longer than the distances between atoms Pt1A and Pt2A, Pt1B and Pt2B, etc (3.2217(3) Å) in the dimers. Intermolecular parallel orientation of dfppy fragments is observed in crystal of **2**. The interplanar distances between the dfppy ligands at platinum atoms Pt1A and Pt1B, Pt1C and Pt1D (3.386 Å) are equal to those in dimers [(dfppy)Pt(pmip)]₂ (3.390 Å) suggesting the intermolecular π ... π stacking interaction between the dfppy ligands.

2.3. Electrochemical properties

The electrochemical properties of Pt(II) complexes **1** and **2** were investigated using cyclic voltammetry (CV) (Fig. 5). The highest occupied molecular orbital (HOMO) and the lowest unoccupied molecular orbital (LUMO) energies for **1** and **2** were calculated using the ferrocene (Cp₂Fe/Cp₂Fe⁺) reference by the equation $E_{\text{HOMO(LUMO)}} = -(4.8 + E^{\text{Ox(Red)}})$ [19]. The energy gap (ΔE) between the HOMO and LUMO can be obtained from these energies. The results for **1** and **2** and also the reported data for parent compounds (ppy)Pt(acac) and (dfppy)Pt(acac) are presented in Table 2.

Fig. 5.**Table 2.**

Both complexes **1** and **2** revealed irreversible anodic and reversible cathodic peaks. A similar redox properties were found previously for parent compounds (ppy)Pt(acac) [13] and (dfppy)Pt(acac) [20]. As anticipated the complex **2** containing a fluorine- substituted ppy ligand is harder oxidized and easier reduced in comparison with **1** containing a non-fluorinated ppy ligand. A similar difference in redox properties were reported for (ppy)Pt(acac) and (dfppy)Pt(acac) compounds [13, 20]. The presence of the pmip ligand at the platinum centre increases the oxidation potentials of complexes **1** and **2** in comparison with the appropriate acac analogs. This can be explained by the fact that the HOMOs in **1** and **2** (vide infra) are localized mainly onto the pmip ligands and they are lower in energy than the corresponding HOMOs in (ppy)Pt(acac) and (dfppy)Pt(acac) complexes which are localized essentially onto arylpyridine ligands [8, 21, 22].

2.4. DFT studies

The molecular geometries of **1** and **2** in the singlet and triplet electronic states were optimized at the B3LYP/def2TZVP level of theory. The computed structures agree well with the X-ray data (e.g. the Pt-N/Pt-C distances are 2.009/1.980 and 2.009/1.976 Å, the OPtO/NPtC angles are 89.3/81.1 and 89.7/81.2° for **1** and **2**, respectively). The HOMO of complexes in the singlet ground state is derived mainly from the pmip orbitals and the Pt d functions (Fig. 6). On the contrary, the LUMO of **1** and **2** is localized on the ppy and dfppy ligand, respectively. The isosurfaces of the frontier orbitals in **1** and **2** are similar but the HOMO of complex **1** is slightly more delocalized onto the ppy ligand as compared to that of compound **2** (Fig. 6). The HOMO-LUMO excitation can be described as an interligand transition for both complexes. The computed HOMO energies (Fig. 6) are lower while the LUMO energies are higher than those derived from the redox potentials (Table 2). This is typical for cycloplatinated complexes and can be explained by the lack of solvation effects in the computations [13]. The HOMO-LUMO energy separation predicted by DFT is very close in **1** and **2** (3.72 and 3.74 eV, respectively) which is in agreement with the results of the CV study (Table 2). On the other hand, the $S_0 - T_1$ energy separation increases from 2.54 to 2.65 eV on going from **1** to **2**. This implies that the $T_1 \rightarrow S_0$ transition involves not only the frontier MOs shown in Fig. 6. Indeed, the calculation of the spin density distribution in the triplet state shows that the unpaired electrons are localized on the Pt-ppy and Pt-dfppy fragment in **1** and **2**, respectively. Correspondingly, the total electron density change accompanying the $T_1 \rightarrow S_0$ transition does not involve the pmip electrons. The

isosurfaces of the spin density and electron deformation density for **1** and **2** are quite similar. They are given in Fig. 7 for complex **1**.

Fig. 6.

Fig. 7.

2.5. Photophysical properties

The absorption spectra of compounds **1** and **2** were measured in CH₂Cl₂ at room temperature and they are shown in Fig. 8. Table 3 summarizes the photophysical data for **1** and **2** and also the reported data for parent Pt compounds - (ppy)Pt(acac) and (dfppy)Pt(acac) for comparison. The spectra of **1** and **2** are similar to those of (ppy)Pt(acac) [4, 14] and (dfppy)Pt(acac) [8]. By analogy with the parent compounds the intense absorption bands in the region of 250-330 nm for both complexes **1** and **2** can be assigned to the π - π^* ligand-centered transition (LC). The lower energy bands below 350 nm are attributed to mixed metal-to-ligand charge-transfer (MLCT) transitions, triplet intraligand (IL) π - π^* transitions and ligand-to-ligand charge-transfer (LLCT) transitions. These assignments correlate well with the MO and electron density isosurfaces obtained from our DFT calculations (Figs. 6, 7). The HOMO-LUMO energy gap derived from the computations corresponds to the wavelength of \sim 330 nm which is in a reasonable agreement with the absorption band positions in the 308-365 nm region (Table 3).

Fig. 8.

Table 3.

Complexes **1** and **2** are luminescent at room temperature both in solution and in solid state. Their photoluminescence (PL) spectra in the degassed CH₂Cl₂ solution (Fig. 9) are similar to those of the acac analogs, (ppy)Pt(acac) and (dfppy)Pt(acac) [3, 4]. The spectra reveal vibronic structures. The spectrum of **1** shows an origin at 489 nm with a vibronic progression of ca. 1250 cm⁻¹ and the spectrum of **2** reveals the 0,0 transition at 471 nm with a vibronic progression of ca. 1310 cm⁻¹. The position of the origin corresponds to the T₁ → S₀ 0,0-transition energy of 2.54 and 2.63 eV for complexes **1** and **2**, respectively. These values are in an excellent agreement with the DFT predictions for the T₁ → S₀ transition energy (2.54 and 2.65 eV, respectively).

Fig. 9.

The structured spectra together with the DFT results suggest that the emissions of **1** and **2** in solution originate from isolated molecules and are attributed to the mixed triplet-singlet LC and MLCT transitions [8, 23]. The incorporation of electronegative fluorine atoms into the 4 and 6 positions of the phenyl ring of the ppy ligand in **2** leads to a blue shift of the emission. A

similar trend was observed for parent compounds (ppy)Pt(acac) and (dfppy)Pt(acac) [4, 23]. The PL quantum yield of **1** (24%) is substantially higher than that of **2** (4%). This correlates with the lower triplet energy level of **1** as compared to **2**. The decrease in the Φ_{em} and τ values on fluorination of the ppy ligand was also observed for the parent platinum complexes [8]. The quantum yields of **1** and **2** are, however, greater than those of (ppy)Pt(acac) and (dfppy)Pt(acac), respectively. This is obviously due to the lower triplet energy of **1** and **2** which decreases the probability of the nonradiative decay involving higher-lying dd^* states [1, 23].

The Pt-Pt interactions between adjacent molecules in crystals of cyclometalated platinum(II) complexes was known to play a crucial role in the formation of excimer emission [3, 21]. As discussed above Pt-Pt interactions between adjacent molecules was not found in crystals of complex **1** and therefore the PL spectrum of **1** in crystalline state contains emission bands of isolated molecules (Fig. 10a).

Fig. 10.

Complex **2** existing in crystalline state as dimeric molecules with obvious Pt-Pt interactions revealed only broad-band red-shifted excimer emission (Fig. 10a). It is interesting to note that the PL spectrum of complex **1** in thin film (Fig. 10b) is similar to the spectrum of **2** and consists of structureless red-shifted broad band which can be assigned to excimer emission. An analogous difference in PL spectra was observed recently for (dfppy)Pt(acac) and related platinum complexes in which the Pt-Pt interactions are absent in crystalline state [3]. The authors explained this phenomenon by the fact that in neat films the molecules of platinum complexes are non-ordered and the formation of adjacent molecules with strong Pt-Pt interactions becomes possible. Apparently the appearance of low-energy broad-band excimer emission in PL spectrum of **1** in neat film can be explained by the same reason.

The preliminary investigations have shown that complexes **1** and **2** can be used as efficient orange emitters in OLEDs.

3. Conclusions

Two novel cyclometalated platinum(II) complexes **1** and **2** with arylpyridine and 1-phenyl-3-methyl-4-isobutyryl-5-pyrazolonate ligands were synthesized. The X-ray diffraction study revealed square-planar geometry for both compounds. Crystal cells were composed from monomer molecules of **1** and from dimeric molecules of **2**. The intense absorption of **1** and **2** in the 250-330 nm region is attributed to the $\pi-\pi^*$ LC transition and the lower intensity bands in the region of 330-430 nm can be assigned to mixed MLCT, IL and LLCT transitions which correlate well with our DFT results. Compounds **1** and **2** are luminescent at room temperature both in

solution and in solid state. The resolved PL spectra in solution originate from the monomer molecules of **1** and **2**, while in crystalline state complex **2** revealed red-shifted broad-band excimer emission originating from dimeric associates of the **2** molecules in crystals. The triplet-state energies of **1** and **2** obtained from the DFT calculations agree very well with the experimental data. The PL quantum yields of **1** and **2** are two times greater than those of the parent compounds (ppy)Pt(acac) and (dfppy)Pt(acac), which gives a ground to consider complexes **1** and **2** as promising emitting materials for OLED devices.

4. Experimental section

4.1. General

All manipulations were carried out in evacuated sealed ampoules or in argon using standard Schlenk techniques. The solvents were thoroughly dried and degassed. All chemicals were received from commercial sources and used without further purification. Platinum(II) chlorides Pt(ppy)(Hppy)(Cl), Pt(4,6-dfppy)(H-4,6-dfppy)(Cl) [24] and sodium pyrazolonate (pmip)Na(DME) [25] were synthesized according to the published procedures.

4.2. Instrumentation

^1H and $^{13}\text{C}\{^1\text{H}\}$ NMR spectra were recorded on a Bruker DPX-200 NMR and on a Bruker Avance III - 400 NMR spectrometers. Compounds were investigated involving Gradient 2D-spectroscopy: proton-proton correlation (GE-COSY) and proton-carbon correlation (GE-HSQC). NMR data are listed in parts per million downfield from TMS. Fourier transform infrared (FTIR) spectra of compounds with KBr pellets were recorded on an IR Fourier spectrometer FSM 1201. Ultraviolet-visible (UV-vis) absorption spectra were recorded on an Perkin Elmer Lambda 25 UV/vis spectrometer. PL spectra were recorded on an Perkin Elmer LS 55 fluorescence spectrometer. Relative PL quantum yields of platinum complexes were measured in degassed CH_2Cl_2 solution with an excitation wavelength of 360 nm using Rhodamine 6G in ethanol ($\Phi_{\text{ref}} = 0.95$) [26] as a reference according to the published literature [27]. Thermogravimetric analysis (TGA) was performed by Perkin Elmer PYRIS 6 TGA thermogravimeter under a dry nitrogen gas flow at a heating rate of 5 °C/min.

In CV studies, a stationary glassy carbon (GC) disc electrode with a working surface of 3.14 mm² was used as the working electrode. The CV curves were recorded in the three-electrode type electrochemical cell in DMF solution in the presence of Bu_4NBF_4 (0.1 M) with a

potential sweep rate of 50 mV s^{-1} using PI-50-1 potentiostat. Silver electrode Ag/AgNO_3 (0.01 M solution in MeCN) was served as the reference electrodes ($E^\circ(\text{Fc}/\text{Fc}^+) = +0.20 \text{ V}$). A Pt wire with a diameter of 1 mm served as the auxiliary electrode. Measurements were carried out in thermostatic conditions ($20 \text{ }^\circ\text{C}$) in nitrogen atmosphere.

4.3. X-ray structural analysis

The X-ray diffraction data for compounds **1** and **2** were collected on a SMART APEX diffractometer (graphite-monochromated, Mo- $K\alpha$ radiation, θ -scan technique, $\lambda = 0.71073 \text{ \AA}$). The intensity data were integrated by the SAINT program [28]. SADABS [29] was used to perform area-detector scaling and absorption corrections. The structures were solved by direct methods and refined on F^2 using all reflections with the SHELXTL package [30]. All non-hydrogen atoms were refined anisotropically. H atoms were located in calculated positions and refined in “the riding-model”. In both dfppy ligands of **2** fluorine atoms were found to be disordered over two positions as well as atoms N(3), C(25) and N(6), C(50). The crystal data and details of the structure determinations for **1** and **2** are summarized in Table 4. Figures 2 and 4 were drawn with Mercury program in ORTEP style [31].

Table 4.

4.4. Computational details

The DFT calculations of the **1** and **2** molecules were performed with use of the Gaussian03 package [32]. The B3LYP hybrid functional [33] was applied together with the def2-TZVP triple- ζ basis set [34] for the optimization of the molecular geometry in the singlet and triplet states. The unrestricted formalism was used for the open-shell T_1 state. The energy of the $T_1 \rightarrow S_0$ 0,0-transition was calculated as a difference between the energies of the triplet and singlet optimized structures. The deformation electron density for the $T_1 \rightarrow S_0$ transition was obtained by subtracting the T_1 total electron density from that of the S_0 state at the optimized geometry of the triplet state.

4.5. Synthesis of complexes

4.5.1. Synthesis of $(\text{ppy})\text{Pt}(\text{pmip})$ (**1**) [35]

To a solution of $\text{Pt}(\text{ppy})(\text{Hppy})(\text{Cl})$ (0.20 g, 0.37 mmol) in 15 ml of DME a solution of $(\text{pmip})\text{Na}(\text{DME})$ (0.13 g, 0.37 mmol) in 5 ml of DME was added under argon atmosphere. The

reaction mixture was heated at 80°C for 16 h, cooled to room temperature and filtered. The solvent was removed under reduced pressure and the residue was recrystallized from CH₂Cl₂ to give **1** as air stable yellow crystalline solid. Yield: 0.16 g (77%). Anal. Calcd for C₂₅H₂₃N₃O₂Pt: C 50.67, H 3.91; Found: C 50.56, H 3.85. FTIR (KBr pellet, ν/cm⁻¹): 3051(m) (ν_{C_{Ar}-H}); 2965(m), 2926(m) (ν_{C_{Alk}-H}); 1607(s), 1376(s) (ν_{C...O}); 1592(s), 1574(s), 1275(s) (ν_{C=C_{Ar}}); 1574(s), 1533(s) (ν_{pyrazolone ring}); 1317(m), 1219(w), 1157(w) (δ_{C-H}); 1095(s), 1059(s), 1030(s), 1000(s), 991(s), 905(m) (δ_{C_{Ar}-H}, ν_{C-C}); 843(m), 751(s) (γ_{C_{Ar}-H}); 692(s), 642(m) (δ_{chelate}); 624(m), 612(w) (ν_{chelate}); 515(m), 494(m), 470(m) (ν_{Pt-O}). According NMR data compound **1** consisted of two isomers around Pt center with the ratio of 70:30. **Major Pt-isomer** (70%) ¹HNMR (200 MHz, CDCl₃, δ, ppm): 9.01 (d, 1H, *J* = 5.3 Hz, ³*J*_{Pt-H} = 44.9 Hz, *Ar*), 7.97 (d, 2H, *J* = 7.6 Hz, *H_o* from Ph), 7.75 (t, 1H, *J* = 7.8 Hz, *Ar*), 7.54 (m, 2H, *Ar*), 7.49 (m, 2H, *H_m* from Ph), 7.38 (m, 1H, *Ar*), 7.30 (t, 1H, *J* = 7.4 Hz, *H_p* from Ph), 7.15 (m, 1H, *Ar*), 7.08 – 7.00 (m, 2H, *Ar*), 3.37 (sept, 1H, *CH* from *iPr*), 2.49 (s, 3H, *Me* from pz), 1.31 (d, 6H, *Me* from *iPr*). **Minor Pt-isomer** (30%) ¹HNMR (200 MHz, CDCl₃, δ, ppm): 8.80 (d, 1H, *J* = 5.2 Hz, ³*J*_{Pt-H} = 45.3 Hz, *Ar*), 7.93 (d, 2H, *J* = 7.5 Hz, *Ar*), 7.86 (d, 1H, *J* = 7.5 Hz, *Ar*), 7.72 – 7.66 (m, 2H, *Ar*), 7.58 – 7.27 (m, 4H, *Ar*), 7.21 (t, 1H, *J* = 7.5, 1H, *Ar*), 7.15 - 7.11 (m, 1H, *Ar*), 7.00 (t, 1H, *J* = 7.3, *Ar*), 3.56 (sept, 1H, *CH* from *iPr*), 2.50 (s, 3H, *Me* from pz), 1.43 (d, 6H, *Me* from *iPr*).

4.5.2. Synthesis of (dfppy)Pt(pmip) (**2**)

To a solution of Pt(4,6-dfppy)(H-4,6-dfppy)(Cl) (0.20 g, 0.33 mmol) in 15 ml of DME a solution of (pmip)Na(DME) (0.12 g, 0.33 mmol) in 5 ml of DME was added under argon atmosphere. The reaction mixture was heated at 80°C for 16 h, cooled to room temperature and filtered. The solvent was removed under reduced pressure and the residue was recrystallized from CH₂Cl₂ to give **2** as air stable orange crystalline solid. Yield: 0.15 g, (71%). Anal. Calcd for C₅₀H₄₂F₄N₆O₄Pt₂: C 47.77, H 3.37; Found: C 47.71, H 3.30. FTIR (KBr pellet, ν/cm⁻¹): 3077(m) (ν_{C_{Ar}-H}); 2965(m), 2926(m) (ν_{C_{Alk}-H}); 1607(s), 1370(s) (ν_{C...O}); 1592(s), 1275(s) (ν_{C=C_{Ar}}); 1577(s), 1533(s) (ν_{pyrazolone ring}); 1305(m), 1249(w), 1163(m) (ν_{C-F}); 1095(s), 1059(s), 1030(m), 1000(m), 985(s), 905(m) (δ_{C_{Ar}-H}, ν_{C-C}); 852(m), 751(s) (γ_{C_{Ar}-H}); 689(m), 660(m) (δ_{chelate}); 624(m), 615(w) (ν_{chelate}); 509(m), 497(m), 470(m) (ν_{Pt-O}). According NMR data compound **2** consisted of two isomers around Pt center with the ratio of 65:35. **Major Pt-isomer** (65%) ¹HNMR (200 MHz, CDCl₃, δ, ppm): 8.95 (d, 1H, *J* = 5.9 Hz, *Ar*), 7.90 (d, 2H, *J* = 8.2, *Ar*), 7.81-7.69 (m, 2H, *Ar*), 7.50-7.40 (m, 2H, *Ar*), 7.32-7.26 (m, 1H, *Ar*), 7.06 (m, 2H, *Ar*), 6.51 (ddd, 1H, *J* = 11.7, 9.3, 2.2 Hz, *Ar*), 3.35 (m, 1H, *CH* from *iPr*), 2.47 (d, 3H, *Me* from pz), 1.29 (d, *Me* from *iPr*). **Minor Pt-isomer** (35%) ¹HNMR (200 MHz, CDCl₃, δ, ppm): 8.78 (d, 1H, *J* = 5.9 Hz,

Ar) and 1.31 (d, *Me* from ¹Pr). [Other signals are overlapped by the resonances of the major isomer].

Acknowledgement

This work was supported by the Russian Foundation for Basic Research (Projects No. 11-03-97021_r_povolzje_a, No. 12-03-00250_a and No. 13-03-00542_a)

Appendix A. Supplementary material

CCDC-914702 (1) and CCDC-914703 (2) contains the supplementary crystallographic data for this paper. These data can be obtained free of charge from The Cambridge Crystallographic Data Center via [www.ccdc.cam.ac.uk/data request/cif](http://www.ccdc.cam.ac.uk/data_request/cif).

References

- [1] J. Kalinowski, V. Fattori, M. Cocchi, J.A. G. Williams, *Coord. Chem. Rev.* 255 (2011) 2401.
- [2] J. A.G. Williams, S. Develay, D. L. Rochester, L. Murphy, *Coord. Chem. Rev.* 252 (2008) 2596.
- [3] C.-H. Chen, F.-I. Wu, Y.-Y. Tsai, C.-H. Cheng, *Adv. Funct. Mater.* 21 (2011) 3150.
- [4] J. Luo, Yu. Liu, D. Shi, Ya. Wang, Z. Zhang, J. Yu, G. Lei, Q. Chen, Ji. Li, X. Deng, W. Zhu *Dalton Trans.* 41 (2012) 1074.
- [5] X. Yang, J. D. Froehlich, H. S. Chae, B. T. Harding, S. Li, A. Mochizuki and G. E. Jabbour, *Chem. Mater.* 22 (2010) 4776.
- [6] E.L. Williams, K. Haavisto, J. Li, G.E. Jabbour, *Adv. Mater.* 19 (2007) 197.
- [7] M. Cocchi, J. Kalinowski, L. Murphy, J.A.G. Williams, V. Fattori, *Org. Electron.* 11 (2010) 388.
- [8] J. Brooks, Ye. Babayan, S. Lamansky, P.I. Djurovich, I. Tsyba, R. Bau, M.E. Thompson, *Inorg. Chem.* 41 (2002) 3055.
- [9] Z. He, W.-Y. Wong, X. Yu, H.-S. Kwok, Z. Lin, *Inorg. Chem.* 45 (2006) 10922.
- [10] W. Wu, C. Cheng, W. Wu, H. Guo, S. Ji, P. Song, K.Han, J.Zhao, Y. Wu, G. Du, *Eur. J. Inorg. Chem.* (2010) 4683.
- [11] G. Zhou, Q. Wang, X. Wang, C.-L. Ho, W.-Y. Wong, D. Ma, L. Wang, Z. Lin, *J. Mater. Chem.* 20 (2010) 7472.
- [12] V. Adamovich, J. Brooks, A. Tamayo, A.M. Alexander, P.I. Djurovich, B.W. D'Andrade, C. Adachi, S.R. Forrest, M.E. Thompson, *New J. Chem.* 26 (2002) 1171.
- [13] M. Ghedini, T. Pugliese, M. La Deda, N. Godbert, I. Aiello, M. Amati, S. Belviso, F. Lelj,

- G. Accorsi, F. Barigelletti, Dalton. Trans. (2008) 4303.
- [14] J. Liu, C.-J. Yang, Q.-Y. Cao, M. Xu, J. Wang, H.-N. Peng, W.-F. Tan, X.-X. Lu, X.-C. Gao, Inorg. Chim. Acta 362 (2009) 575.
- [15] X. Mou, Y. Wu, S. Liu, M. Shi, X. Liu, C. Wang, S. Sun, Q. Zhao, X. Zhou, W. Huang, J. Mater. Chem. 21 (2011) 13951.
- [16] J. Deng, Y. Wang, X. Li, M. Ni, M. Liu, Y. Liu, G. Lei, M. Zhu, W. Zhu, Chin. J. Chem. 29 (2011) 2057.
- [17] S.S. Batsanov, Russ. J. Inorg. Chem. 36 (1991) 1694.
- [18] C. Janiak, J. Chem. Soc., Dalton Trans. (2000) 3885.
- [19] M. Thelakkat, H.-W. Schmidt, Adv. Mater. 10 (1998) 219.
- [20] B. Ma, P.I. Djurovich, M.E. Thompson, Coord. Chem. Rev. 249 (2005) 1501.
- [21] D. Kim, J.-L. Brédas, J. Am. Chem. Soc. 131 (2009) 11371.
- [22] M. Zhang, Y. Li, Z.-S. Li, J.-Z. Sun, Int. J. Quantum Chem. 110 (2010) 1142.
- [23] A.F. Rausch, L. Murphy, J.A.G. Williams, H. Yersin, Inorg. Chem. 51 (2012) 312.
- [24] J.-Ya. Cho, K. Yu. Saponitsky, J. Li, T.V. Timofeeva, S. Barlow, S.R. Marder, J. Organomet. Chem. 690 (2005) 4090.
- [25] E.O. Platonova, E.V. Baranov, L.N. Bochkarev, Yu.A. Kurskii, Russ. J. Coord. Chem. 38 (2012) 696.
- [26] B. Li, W.R. Miao, L.B. Cheng, Dyes Pigments 43 (1999) 161.
- [27] J.N. Demas, G.A. Crosby, J. Phys. Chem. 75 (1971) 991.
- [28] SAINTPlus Data Reduction and Correction Program, v. 6.02a; Bruker AXS: Madison, WI, 2000.
- [29] G.M. Sheldrick, SADABS, v. 2.01, Bruker/Siemens Area Detector Absorption Correction Program; Bruker AXS: Madison, WI, 1998.
- [30] G.M. Sheldrick, SHELXTL, v. 6.12, Structure Determination Software Suite; Bruker AXS: Madison, WI, 2000.
- [31] C.F. Macrae, P.R. Edgington, P. McCabe, E. Pidcock, G.P. Shields, R. Taylor, M. Towler, J. van de Streek, J. Appl. Cryst. 39 (2006) 453.
- [32] M. J. Frisch, G. W. Trucks, H. B. Schlegel, G. E. Scuseria, M. A. Robb, J. R. Cheeseman, J. A. Montgomery, Jr., T. Vreven, K. N. Kudin, J. C. Burant, J. M. Millam, S. S. Iyengar, J. Tomasi, V. Barone, B. Mennucci, M. Cossi, G. Scalmani, N. Rega, G. A. Petersson, H. Nakatsuji, M. Hada, M. Ehara, K. Toyota, R. Fukuda, J. Hasegawa, M. Ishida, T. Nakajima, Y. Honda, O. Kitao, H. Nakai, M. Klene, X. Li, J. E. Knox, H. P. Hratchian, J. B. Cross, V. Bakken, C. Adamo, J. Jaramillo, R. Gomperts, R. E. Stratmann, O. Yazyev, A. J. Austin, R. Cammi, C. Pomelli, J. W. Ochterski, P. Y. Ayala, K. Morokuma, G. A. Voth, P. Salvador, J.

J. Dannenberg, V. G. Zakrzewski, S. Dapprich, A. D. Daniels, M. C. Strain, O. Farkas, D. K. Malick, A. D. Rabuck, K. Raghavachari, J. B. Foresman, J. V. Ortiz, Q. Cui, A. G. Baboul, S. Clifford, J. Cioslowski, B. B. Stefanov, G. Liu, A. Liashenko, P. Piskorz, I. Komaromi, R. L. Martin, D. J. Fox, T. Keith, M. A. Al-Laham, C. Y. Peng, A. Nanayakkara, M. Challacombe, P. M. W. Gill, B. Johnson, W. Chen, M. W. Wong, C. Gonzalez, and J. A. Pople, Gaussian 03, Revision D.01, Gaussian, Inc., Wallingford CT, 2004

[33] A. D. Becke, *J. Chem. Phys.* 98 (1993) 5648-52.

[34] F. Weigend, R. Ahlrichs, *Phys. Chem. Chem. Phys.*, 2005, 7, 3297

[35] Preliminary communication: Yu.E. Begantsova, L.N. Bochkarev, V.A. Ilichev, M.N. Bochkarev, *Russ. Chem. Bull.* № 8 (2012) 1654.

Captions to Figures and Tables:

Fig. 1. Molecular structure of **1** with thermal ellipsoids of 30% probability.

Fig. 2. Fragments of crystal packing of **1** in projection on the plane a_0c (*a*) and a_0b (*b*) (50% ellipsoid probability, H atoms are omitted).

Fig. 3. Molecular structure of **2** with thermal ellipsoids of 30% probability. Me groups of *i*-Pr substituents are omitted for clarity.

Fig. 4. Fragments of crystal packing of **2** (50% ellipsoid probability, H atoms are omitted).

Fig. 5. Cyclic voltammograms of complexes **1** and **2** in DMF ($5 \times 10^{-3} M$), scan rate = 50 mV s^{-1} (CV curves were recorded at the first scan from 0.00 V to -2.40 V then back to 0.70 V and to 0.00 V).

Fig. 6. Isosurfaces (the isovalue is 0.02 a.u.) of the HOMO (left) and LUMO (right) for complex **1** (top) and **2** (bottom). The hydrogen atoms are omitted for clarity. The orbital energies calculated at the B3LYP/def2TZVP level of theory are given.

Fig. 7. The spin density (left) and the $T_1 \rightarrow S_0$ deformation electron density (right) isosurfaces (the isovalue is 0.0004 a.u.) for complex **1**. The hydrogen atoms are omitted for clarity.

Fig. 8. Absorption spectra of **1** and **2** in CH_2Cl_2 ($10^{-5} \text{ mol L}^{-1}$).

Fig. 9. PL spectra of **1** and **2** in CH_2Cl_2 at room temperature ($10^{-5} \text{ mol L}^{-1}$) ($\lambda_{\text{ex}} = 360 \text{ nm}$).

Fig. 10. PL spectra of **1** and **2** in crystalline states (a) and in films (b) measured at room temperature ($\lambda_{\text{ex}} = 360 \text{ nm}$).

Table 1. Selected bond distances (\AA) and angles ($^\circ$) in **1** and **2**.

Table 2. Redox properties and frontier orbital energies of platinum(II) complexes.

Table 3. Photophysical properties of platinum(II) complexes at room temperature.

Table 4. Crystallographic data of **1** and **2**.

ACCEPTED MANUSCRIPT

New cyclometalated platinum(II) complexes with pyrazolonate ancillary ligand were synthesized and structurally characterized. Their electrochemical and photophysical properties were investigated and DFT calculations were performed.

ACCEPTED MANUSCRIPT

Table 1. Selected bond distances (Å) and angles (°) in **1** and **2**.

Bond, Å	1	2
Pt(1)-O(1)	2.035(3)	2.057(3)
Pt(1)-O(2)	2.077(3)	2.066(3)
Pt(1)-C(25)	1.982(4)	1.969(4)
Pt(1)-N(3)	1.980(4)	1.971(3)
O(1)-C(1)	1.274(5)	1.278(5)
O(2)-C(3)	1.269(5)	1.258(5)
C(1)-C(2)	1.439(6)	1.426(6)
C(2)-C(3)	1.419(6)	1.413(6)
Pt(2)-O(3)	-	2.030(3)
Pt(2)-O(4)	-	2.069(3)
Pt(2)-C(50)	-	1.957(4)
Pt(2)-N(6)	-	1.964(3)
O(3)-C(26)	-	1.282(4)
O(4)-C(28)	-	1.273(5)
C(26)-C(27)	-	1.424(5)
C(27)-C(28)	-	1.409(5)
Pt(1)-Pt(2)	-	3.2217(3)
Angle, °		
O(1)-Pt(1)-O(2)	91.92(11)	91.70(11)
C(25)-Pt(1)-N(3)	81.81(18)	81.30(12)
O(1)-Pt(1)-N(3)	175.36(15)	174.79(12)
O(2)-Pt(1)-C(25)	173.93(14)	173.54(12)
O(3)-Pt(2)-O(4)	-	90.99(10)
C(50)-Pt(2)-N(6)	-	81.22(12)
O(3)-Pt(1)-N(6)		175.82(11)
O(4)-Pt(1)-C(50)		174.23(11)

Table 2. Redox properties and frontier orbital energies of platinum(II) complexes

Compound	E_p^{red} (V)	E_p^{ox} (V)	HOMO (eV)	LUMO (eV)	ΔE (eV)
1	-2.20	0.52	-5.32	-2.60	2.72
2	-2.11	0.59	-5.39	-2.69	2.70
(ppy)Pt(acac)	-2.40 ^a	0.34 ^a	-5.14	-2.40	2.74
(dfppy)Pt(acac)	-2.29 ^b	0.52 ^b	5.32	-2.51	2.81

^a [13]; ^b [20];

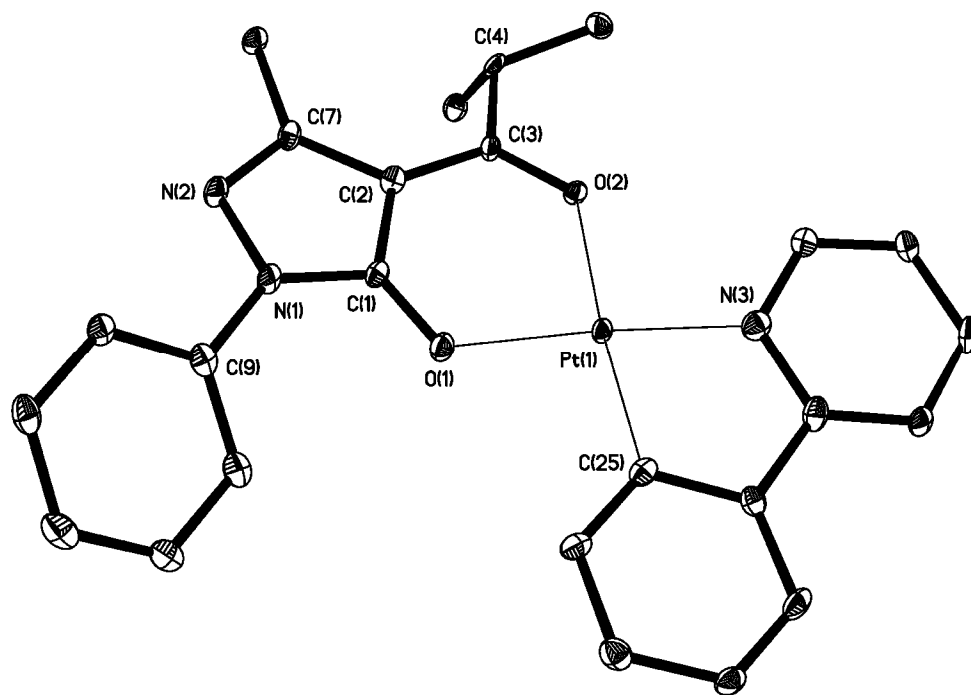
Table 3. Photophysical properties of platinum(II) complexes at room temperature

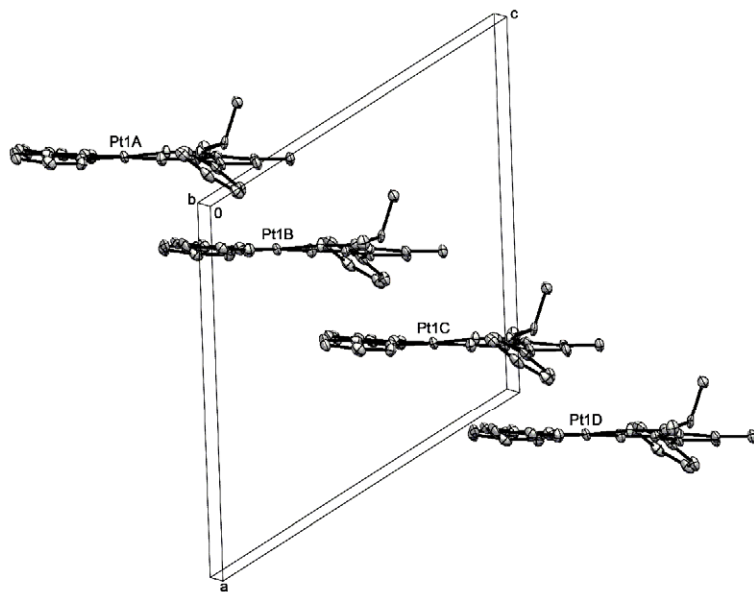
Complex	$\lambda_{\text{abs}}/\text{nm}$ ($10^{-4}\epsilon_{\text{max}}$ / $\text{M}^{-1}\text{cm}^{-1}$)	$\lambda_{\text{em}}/\text{nm}$ (solution)	$\Phi_{\text{em}}/\%$ (solution)	$\lambda_{\text{em}}/\text{nm}$ (film)	$\lambda_{\text{em}}/\text{nm}$ (crystal)
1	256 (35.2), 283 (21.3), 313 (12.0), 327 (10.0), 365 (7.4), 405 sh (1.9)	489, 521, 560 sh	24	589	487, 512, 543
2	255 (32.5), 284 sh (19.2), 308 (10.8), 321 (8.9), 359 (6.3), 382 sh (2.4)	471, 502, 530 sh	4	578	584
(ppy)Pt(acac) ^a	250 (33.2), 277 (23.8), 313 (11.6), 327 (10.4), 347 (6.2), 364 (6.9), 410 (1.8), 430 (0.18)	484, 515	15	500, 528, 570	-
(dfppy)Pt(acac) ^b	252 (30), 273 sh (19), 308 (11), 321 (11), 359 (6.9), 390 sh (2.4)	467	2	616	-

^a [4, 8, 14]; ^b [3, 8, 23]

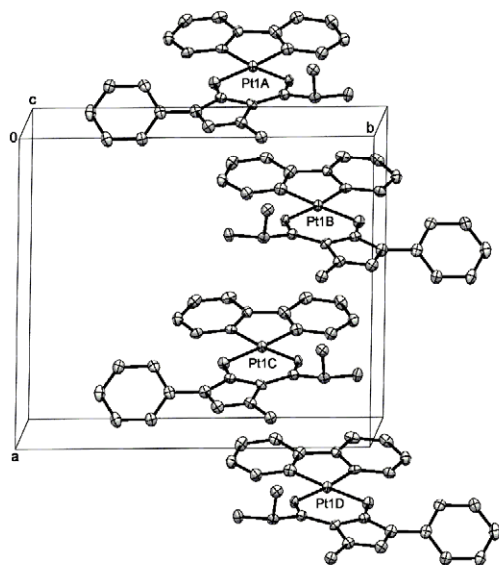
Table 4. Crystallographic data of **1** and **2**.

	compound 1	compound 2
Empirical formula	C ₂₅ H ₂₃ N ₃ O ₂ Pt	C ₅₀ H ₄₂ F ₄ N ₆ O ₄ Pt ₂
Formula weight	592.55	1257.08
Temperature, K	100(2)	100(2)
Wavelength, Å	0.71073	0.71073
Crystal system	Monoclinic	Monoclinic
Space group	Cc	P2(1)/c
Unit cell dimensions	a = 13.6462(16) Å ; $\alpha = 90^\circ$	a = 14.6651(9) Å, $\alpha = 90^\circ$
	b = 14.0309(17) Å, $\beta = 120.640(2)^\circ$	b = 12.8491(8) Å, $\beta = 100.9430(10)^\circ$
	c = 12.7707(16) Å, $\gamma = 90^\circ$	c = 23.0378(14) Å, $\gamma = 90^\circ$
Volume, Å ³	2103.8(4)	4262.2(5)
Z	4	4
Density (calculated), Mg/m ³	1.871	1.959
Absorption coefficient, mm ⁻¹	6.698	6.631
F(000)	1152	2432
Crystal size, mm	0.38 × 0.21 × 0.15	0.24 × 0.20 × 0.10
Theta range for data collection	2.26 - 26.50°	1.41 - 26.00°
Completeness to $\theta = 26.00$	99.5 %	97.7 %
Reflections collected	6319	24561
Independent reflections	3670 [R(int) = 0.0334]	8198 [R(int) = 0.0373]
Absorption correction	Semi-empirical from equivalents	Semi-empirical from equivalents
Refinement method	Full-matrix least-squares on F ²	Full-matrix least-squares on F ²
Data / restraints / parameters	3670 / 8 / 283	8198 / 62 / 614
Final R indices [I > 2 σ (I)]	R1 = 0.0309, wR2 = 0.0740	R1 = 0.0348, wR2 = 0.0762
R indices (all data)	R1 = 0.0315, wR2 = 0.0744	R1 = 0.0444, wR2 = 0.0792
Goodness-of-fit on F ²	1.016	1.054
Absolute structure parameter	-0.001(10)	-
Largest diff. peak and hole, e·Å ⁻³	2.941; -2.242	1.419; -1.788

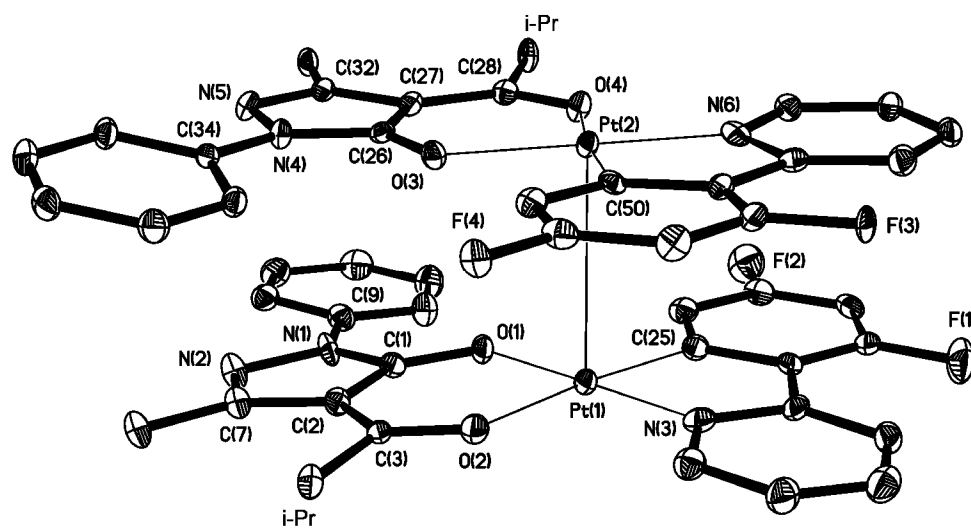


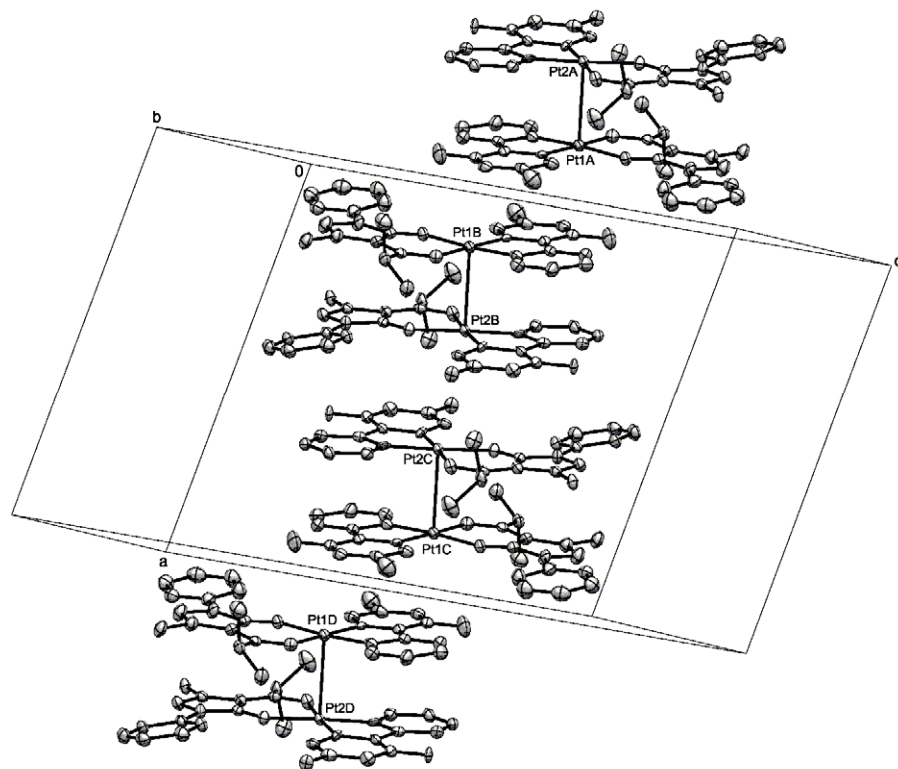


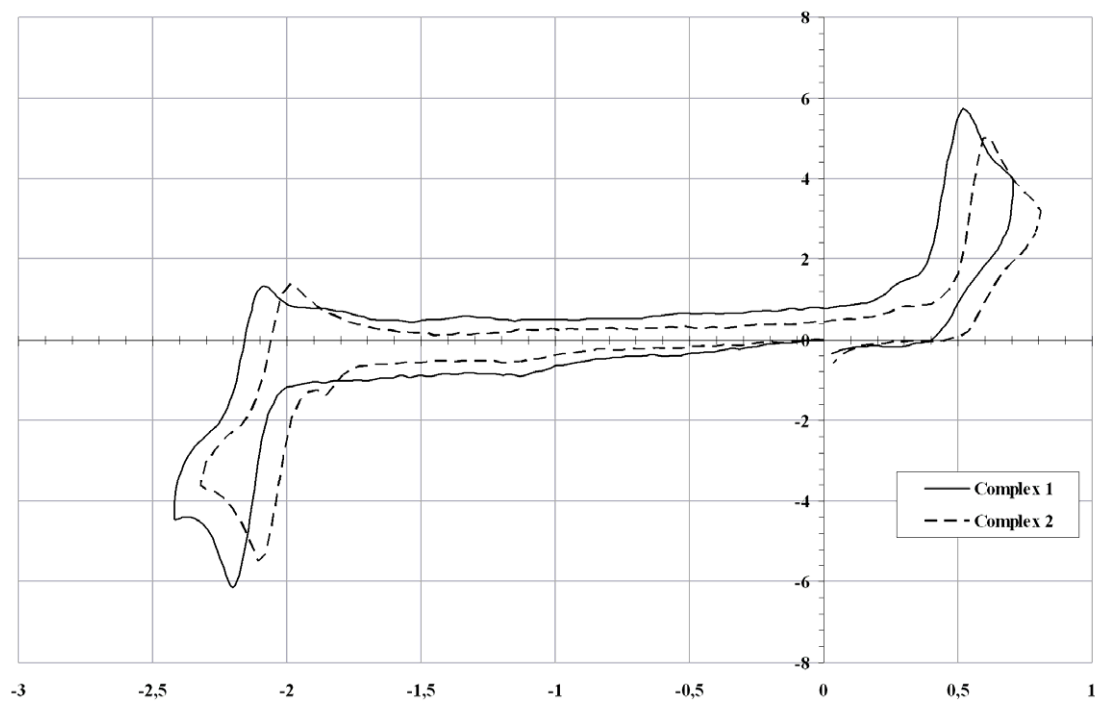
a

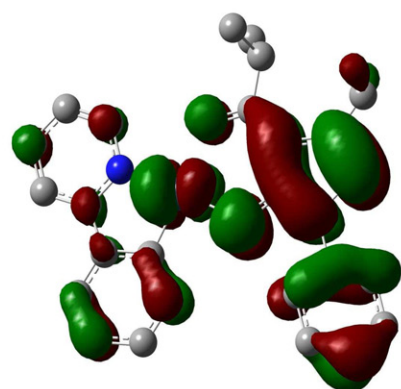


b

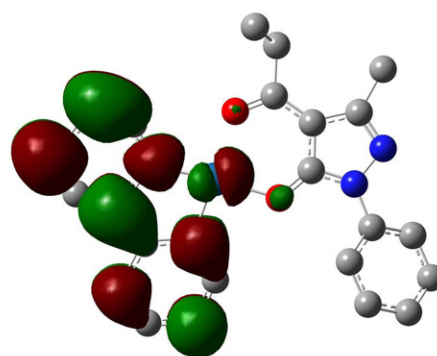
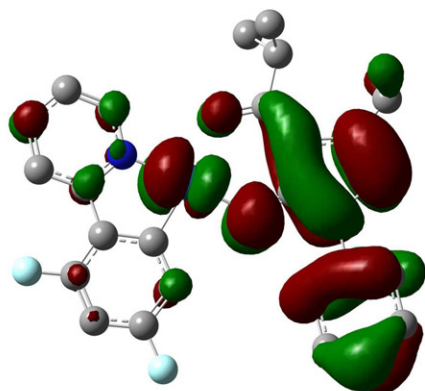




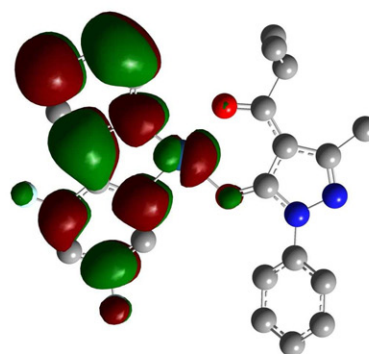


 $E_{\text{HOMO}} = -5.70 \text{ eV}$

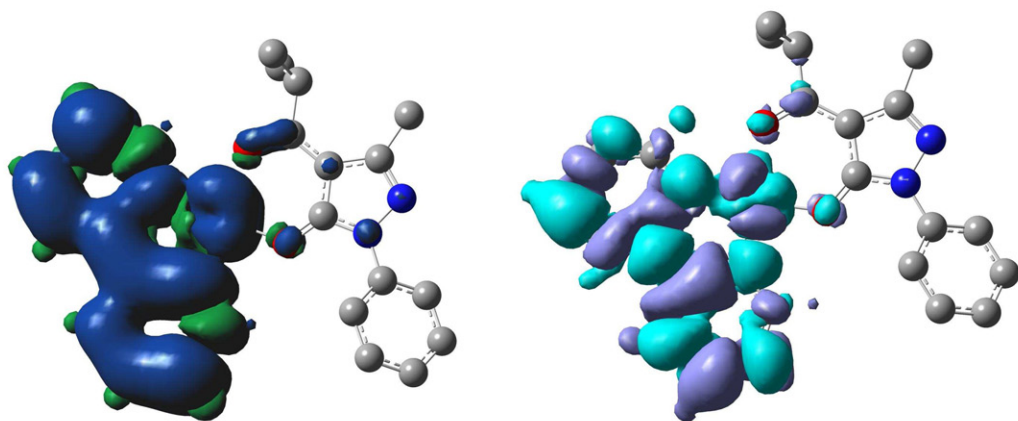
(ppy)Pt(pmip)

 $E_{\text{LUMO}} = -1.98 \text{ eV}$  $E_{\text{HOMO}} = -5.85 \text{ eV}$

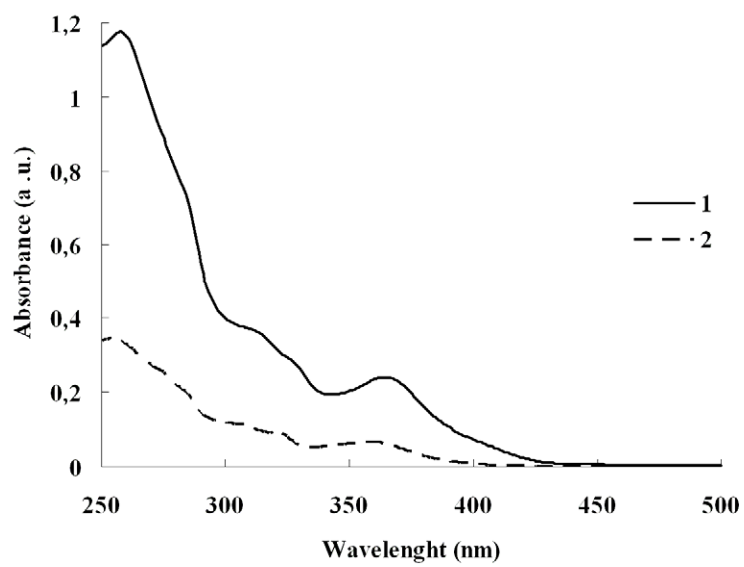
(dfppy)Pt(pmip)

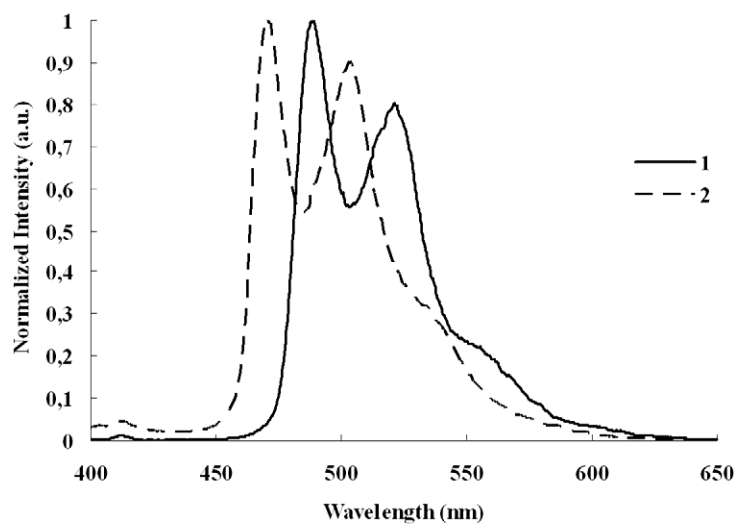
 $E_{\text{LUMO}} = -2.11 \text{ eV}$

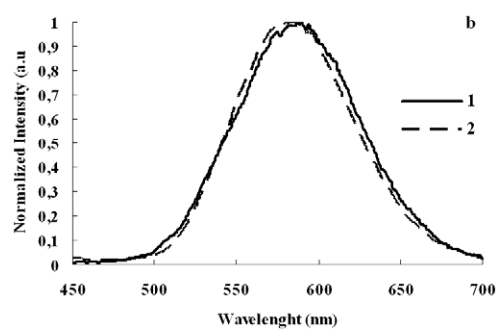
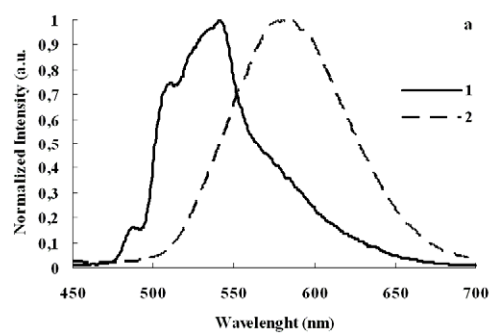
ACCEPTED



ACCEPTED MANUSCRIPT







ACCEPTED MANUSCRIPT